Eur. Phys. J. D **23**, 285–290 (2003)
DOI: 10.1140/epjd/e2003-00042-8

THE EUROPEAN PHYSICAL JOURNAL D

Photorefractive ac-enhanced nonlinear response of sillenites: Low- and high-contrast effects

O. Filippov[1,a], K.H. Ringhofer[1,†], and B.I. Sturman[2]

[1] Physics Department of the University, 49069 Osnabrück, Germany
[2] International Institute for Nonlinear Studies, Koptyg Ave 1, 630090, Novosibirsk, Russia

Received 13 September 2002 / Received in final form 27 December 2002
Published online 11 February 2003 –

Abstract. Analytically and numerically we investigate the dependence of the first Fourier harmonics of the space-charge field, induced in an AC-biased sillenite crystal by a light-interference pattern, on the light contrast m. It is shown that within the whole contrast range, $0 < m < 1$, these dependences are controlled by the only scalar parameter – the space-charge wave quality factor Q. In the low-contrast limit, $m \lesssim Q^{-2}$, this factor defines the degree of enhancement of the nonlinear response while for larger contrasts it characterizes strong saturation effects. The data obtained are compared with the results of the previous studies of the AC-response. The possibilities of experimental detection of predicted dependences and their possible implications are discussed.

PACS. 42.65.Ky Frequency conversion; harmonic generation, including higher-order harmonic generation – 78.20.Bh Theory, models, and numerical simulation

1 Introduction

The idea of AC-enhancement of the insufficiently high nonlinear response of fast photorefractive crystals (the sillenites $Bi_{12}SiO_{20}$, $Bi_{12}TiO_{20}$, $Bi_{12}GeO_{20}$, the semiconductors GaAs, GaP, etc.) goes back to the 80s [1,2]. It was found first in 1985 [3] that employment of a quickly oscillating electric AC-field is able to increase the light-induced space-charge field within the low-contrast limit and to make the photorefractive response non-local, *i.e.*, gradient-like. Such a non-local response is convenient for many practical purposes.

In the subsequent years the AC-enhancement technique had become the subject of numerous experimental and theoretical studies. It was found, in particular, that a square-wave shape of the AC-field provides the best enhancement [4], that the low-contrast range, where the fundamental component of the space-charge field grows linearly with m is very narrow, and that the enhancement property is closely related to the presence of weakly damped, low-frequency eigenmodes – space-charge waves [5] – and to the generation of spatial subharmonics [1]. The large-contrast AC-effects in the sillenites were investigated in [6,7].

During the last decade, large applied fields (up to 50 kV/cm [8,9]) have become available for AC-experiments. Furthermore the region of large light contrast has become important in connection with the soliton propagation problem [10]. Lastly, a number of applications of fast photorefractive materials, such as detection of weak signals, are relevant to the high-contrast effects [11–13]. It was found recently under rather general conditions that the space-charge field induced in a fast AC-biased crystal by a finite light beam possesses a discontinuity [14,15]. The width of this discontinuity lies in the sub-μm range, it is much smaller than the typical scale of light-intensity variations.

Below, after ten years, we revisit the problem of high-contrast AC-response of fast photorefractive crystals. In contrast to [6,7] we do not restrict ourselves to the fundamental component of the space-charge field. We account for the discontinuity of the field profile and work in the terms providing generality of the results obtained. Finally, we address the problems related to measurements of the spatial harmonics and applications of the nonlinear AC-response.

It should be noted that apart from the AC-technique for enhancement of the photorefractive response the so-called DC-technique [1,16] (which requires application of a DC electric field and an introduction of a frequency detuning between the light beams) was also the subject of many studies. The problem of high-contrast DC-response was considered in [17,18]. It is quite different in physics from the problem in question.

[a] e-mail: oleg.filippo@uni-osnabrueck.de
† This author dead in December 26, 2002.

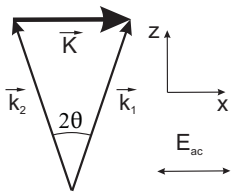

Fig. 1. Geometrical diagram of an AC experiment.

Lastly, we mention that the high-contrast effects are important also for cubic InP crystals [29,30]. However, the charge transport processes are essentially different in this case from the processes relevant to the sillenites.

2 Basic relations

We assume that two light waves propagate symmetrically to the z-axis in a fast photorefractive crystal and a square-wave AC-field is applied parallel to the x-axis, see Figure 1. The vectorial complex amplitudes of the light waves we denote $\mathbf{a}_{1,2}$. They can change with z because of the linear (field-induced birefringence and optical activity) and nonlinear (energy exchange) effects. The sum $|\mathbf{a}_1|^2+|\mathbf{a}_1|^2$, which is proportional to the total intensity, does not depend on z. From now on we normalize the vectorial amplitudes in such a way that this sum equals to unity.

The spatially modulated part of the intensity distribution, $\tilde{I}$, produced by these two waves and normalized to the sum of their intensities is

$$\tilde{I} = (\mathbf{a}_2^* \cdot \mathbf{a}_1)\, \exp(\mathrm{i}Kx) + \text{c.c.}, \qquad (1)$$

where $K = |\mathbf{k}_1 - \mathbf{k}_2|$ is the absolute value of the light wavevector difference (often called the grating vector), x is the fringe coordinate measured in the direction of the vector $\mathbf{k}_1 - \mathbf{k}_2$, and c.c. stands for complex conjugation. The contrast of the interference light pattern, m, is given by $m = 2|\mathbf{a}_2^* \cdot \mathbf{a}_1|$. The presence of the scalar product in equation (1) and in the definition of m is important for optically isotropic cubic crystals. The polarization states of light waves change here because of nonlinear coupling and this change cannot be generally separated from the intensity changes [19,20]. The contrast m reaches its maximum value (unity) only for equal intensities, $|\mathbf{a}_1|^2 = |\mathbf{a}_2|^2 = 1/2$, and identical polarization states, $\mathbf{a}_1 \parallel \mathbf{a}_2$. As clear from equation (1), the intensity distribution $\tilde{I}$ can be rewritten in the real form, $\tilde{I} = m\cos(Kx + \varphi)$ with $\varphi = \arg(\mathbf{a}_2^* \cdot \mathbf{a}_1)$. Generally, the phase φ depends on the propagation coordinate z because of coupling effects and this dependence is important for description of the vectorial 2W-coupling.

The light-induced space-charge field E_{sc} is directed along the x-axis and can be presented in the form

$$E_{\mathrm{sc}}(x) = E_1\, \mathrm{e}^{\mathrm{i}(Kx+\varphi)} + E_2\, \mathrm{e}^{2\mathrm{i}(Kx+\varphi)} + \ldots + \text{c. c.}, \qquad (2)$$

The amplitudes E_1, E_2, ... are complex functions of m; the form of these functions depends on the charge transport mechanism. The fundamental amplitude E_1 is of prime importance for photorefractive effects because it characterizes the rate of mutual Bragg diffraction of the recording beams and, therefore, the coupling strength during 2W-coupling.

In the case under study the charge separation occurs under an alternating external AC-field. This field is assumed to be parallel to the x-axis, to change periodically its sign, $E_{\mathrm{ex}}(t) = \pm E_0$, and have an oscillation period much smaller than the photorefractive response time. These conditions provide an optimum AC-enhancement [4]. In experiment, the amplitude E_0 is often larger than (or comparable with) 10 kV/cm. Diffusion charge separation is negligible in this case.

The high speed of the AC-oscillations allows to employ an averaging procedure to find the static profile $E_{\mathrm{sc}}(x)$. This procedure was used first within the low contrast approximation (and within the conventional one-species model of charge transfer) to find the first spatial harmonic E_1 [3]. The main result of this paper we present in a form which is convenient for what follows,

$$E_1/E_0 \simeq -\mathrm{i}\, m\, Q/2\,, \qquad (3)$$

where the real quantity $Q = Q(K, E_0)$ is the quality factor for the space-charge wave with wavevector K [5],

$$Q = \left(\frac{E_0}{E_q} + \frac{E_m}{E_0} + \frac{E_d}{E_0}\right)^{-1}, \qquad (4)$$

E_q, E_m, and E_d are the conventional characteristic fields [1,2],

$$E_q = \frac{qN_t}{\epsilon\epsilon_0 K}\,, \qquad E_m = \frac{1}{K\mu\tau}\,, \qquad E_d = \frac{Kk_bT}{q}\,, \qquad (5)$$

q is the elementary charge, N_t the effective trap concentration, $\epsilon\epsilon_0$ the static dielectric constant, $\mu\tau$ the mobility-lifetime product for photo-excited electrons, k_b the Boltzman constant, and T the absolute temperature.

The maximum value of the function $Q(K, E_0)$ is $(qN_t\mu\tau/4\epsilon\epsilon_0)^{1/2}$ [5]. The fast photorefractive crystals are distinguished by large values of the $\mu\tau$-product, here $Q_{\max} \gg 1$. With the values $N_t = 2\times10^{16}$ cm^{-3}, $\mu\tau = 3\times10^{-7}$ cm^2/V, and $\epsilon\epsilon_0 = 50$, representative for the sillenites, we have $Q_{\max} \simeq 8$.

The most important features of the dependence $Q(K, E_0)$ can be described as follows. For E_0 considerably larger than $(N_tk_bT/\epsilon\epsilon_0)^{1/2}$ (which is typically of the order of a few kV/cm) the diffusion contribution to Q [the last term in Eq. (4)] can be neglected. In this case, the optimum value of the grating vector, $K_{\mathrm{opt}} \simeq E_0^{-1}\,(qN_t/\epsilon\epsilon_0\mu\tau)^{1/2}$ and the corresponding peak value of $Q(K)$ is not far from $Q_{\max}$. This is illustrated by Figure 2 for the above representative material parameters. Note that for $E_0 \sim 10^1$ kV/cm the optimum value of K corresponds to half-angle θ between the incident light beams (see Fig. 1) of the order of a few degrees. The larger E_0, the wider (in Λ) is the region of large Q. The presence of the AC-enhancement manifests itself clearly in experiments on light-induced scattering in the sillenites [20–22]: the strongest scattering angles correspond to K_{opt}.

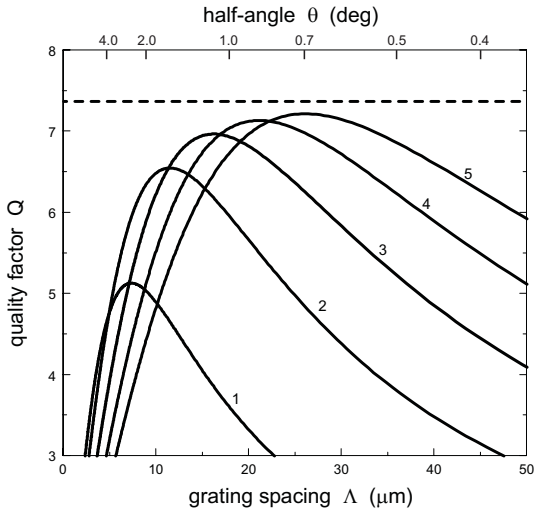

Fig. 2. Dependence $Q(\Lambda)$ for $\epsilon\epsilon_0 = 50$, $N_t = 2 \times 10^{16}$ cm^{-3}, $\mu\tau = 3 \times 10^{-7}$ cm^2/V, and several values of E_0. The curves 1, 2, 3, 4, and 5 correspond to $E_0 = 4$, 8, 12, 16 and 20 kV/cm, respectively. The dashed line shows the value of $Q_{\max}$ for the accepted material parameters.

The introduced quality factor has also an apparently different implication. It defines the threshold of the so-called subharmonic generation in the sillenites, which corresponds to the parametric instability against excitation of weakly damped space-charge waves [5,23]. Lastly we mention that the quality factor can be directly measured in experiment [24].

Let us return to equation (3) valid in the low contrast approximation. The presence of the imaginary unit i means that the photorefractive response is non-local, *i.e.*, the light and field fringes are shifted to each other by a quarter of a period.

Since the amplitude of the space-charge field related to the first Fourier harmonic is $2|E_1|$, we have $E_{\rm sc}^{(1)}/E_0 \simeq mQ$. Hence already at $m \approx Q^{-1} \ll 1$, the space-charge field becomes comparable with the applied field. The linear approximation (ignoring the material nonlinearity) is clearly broken here. This situation differs strongly from that typical for slow ferroelectrics, which is caused by the difference in values of the lifetime-mobility product for photo-excited charge carriers [5].

Recently, the procedure of averaging over the fast AC-oscillations was applied to the nonlinear case (an arbitrary light contrast) to obtain a simple differential equation for the normalized space-charge field $e = E_{\rm sc}(x)/E_0$ in the diffusion-free limit $E_0 \gg (N_t k_b T/\epsilon\epsilon_0)^{1/2}$. This ordinary second-order equation reads [14],

$$\left[\frac{(e^2-1)\,(1+\tilde{I})}{1+l_s\,e_x}\right]_x = \frac{e\,(1+\tilde{I})}{l_0}, \qquad (6)$$

where the subscript x denotes the x-differentiation, $l_0 = \mu\tau E_0$ is the characteristic drift length, and $l_s = \epsilon\epsilon_0 E_0/qN_t$ the characteristic saturation length. For representative parameters of the sillenites and $E_0 = 20$ kV/cm we have the estimates, $l_0 \approx 50$ μm, $l_s \approx 0.4$ μm. Correspondingly, the grating vector K has to range between l_0^{-1} and l_s^{-1} to meet the requirement $Q \gg 1$.

Within the linear approximation in $\tilde{I}$ we have from here $l_0 l_s e_{xx} - e = l_0 \tilde{I}_x$ and for the first harmonic E_1 we return immediately to equation (3). In the general case, an even intensity distribution $\tilde{I}(x)$ produces an odd distribution $e(x)$.

The distinctive feature of equation (6) is the presence of the smallest characteristic length l_s before the derivative e_x in the denominator. As soon as the nonlinear (in m) terms become important, this feature causes a highly peculiar behavior of the field profile $e(x)$. Namely, this profile cannot be smooth on the scale of the grating period $\Lambda = 2\pi/K$, it has to include a discontinuity of $e(x)$. If we assume the opposite, the term $l_s e_x$ can be neglected; then equation (6) becomes a first-order differential equation which cannot possess any periodic solution for e. Therefore the solution of equation (6) must possess discontinuities. Their width can be estimated as $\approx l_s$. Note that the presence of a small coefficient before the highest (second) derivative is typical, *e.g.*, of Burgers equations which describes shock waves in hydrodynamics [25].

3 Results

Recently, equation (6) was applied to the beam propagation problem [15]. Below we use it to describe the characteristics of light-induced gratings arising during 2W-mixing. Correspondingly, the intensity distribution $\tilde{I}$ was chosen in the form $\tilde{I} = m\cos(Kx)$.

Apart from the low-contrast limit, equation (6) cannot be solved analytically. To solve it numerically, we have used the standard procedure **b**vp4c of the package MATLAB 6.0. Starting from $m = 0$, we increased the contrast with the increment 5×10^{-4} using the solution obtained in the kth step as the "hypothesis" for the next $(k+1)$th step. The steps in x have been chosen automatically to ensure the relative accuracy 10^{-3}. With Pentium 4 of 2 GHz, the calculations performed were not time-consuming.

Figure 3 shows the main tendencies in the change of the space-charge field profile with increasing contrast for $Q \approx 6$. One sees that a sine-like profile occurs only for $m \lesssim 0.05$. With increasing m, the discontinuity (situated at the intensity maximum) quickly progresses; far from the discontinuity the function $e(x)$ experiences a strong saturation and approaches the square-wave form $e = \pm 1$. The light-induced field never exceeds the applied field, $|E_{\rm sc}| < E_0$. It is curious that a strong steepening of the field profile at the intensity minima ($x/\Lambda \simeq \pm 0.5$) occurs only when m is approaching unity.

Since the function $e(x)$ is odd, all its Fourier harmonics are imaginary,

$$e_n(m) \equiv \frac{E_n(m)}{E_0} = -2\mathrm{i}\int_0^{1/2} e(\xi, m)\sin(2\pi n\xi)\,\mathrm{d}\xi, \qquad (7)$$

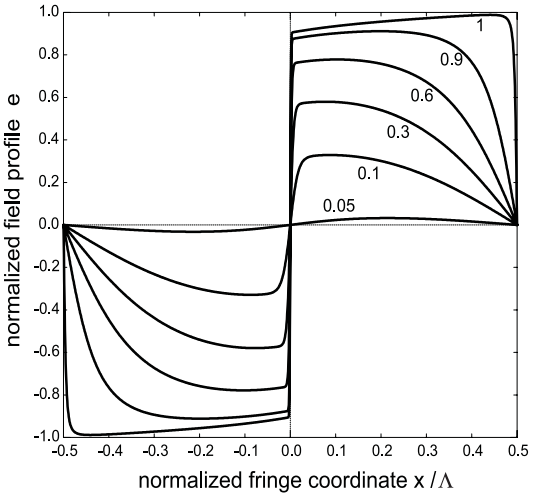

Fig. 3. The profile $e(x)$ for the accepted material parameters, $E_0 = 13$ kV/cm, $\Lambda = 30$ μm, ($Q \simeq 6.2$), and several values of the contrast. The curves 1, 2, 3, 4, 5, and 6 correspond to $m = 0.05$, 0.1, 0.3, 0.6, 0.9, and 1.0, respectively.

with $\xi = x/\Lambda$. This means, in particularly, that the fundamental component of $E_{\rm sc}(x)$ is $\pi/2$-shifted with respect to the intensity distribution for any value of the contrast, *i.e.*, the photorefractive AC-response is always non-local. Using the approximation of a square-wave profile of $e(x)$ for $m = 1$, we obtain the following estimate of the limit values of the spatial harmonics: $e_n(1) \simeq -2\mathrm{i}/n\pi$ for odd numbers ($n = 1, 3, ...$) and $e_n(1) = 0$ for even numbers, ($n = 2, 4, ...$). For the fundamental component we expect, therefore, the limit value $|e_1(m = 1)| \simeq 2/\pi \simeq 0.64$.

For what follows it is useful to represent the dependence $e_1(m) \equiv E_1(m)/E_0$ in the form

$$e_1 = -(\mathrm{i}mQ/2)\, F_1 \,, \qquad (8)$$

where $F_1(m)$ is a dimensional function with a unit initial value, $F_1(0) = 1$. While using equation (8) for the description of the vectorial coupling [20,22], it is important to keep the phase factor $\exp(\mathrm{i}\varphi) = 2(\mathbf{a}_2^* \cdot \mathbf{a}_1)/m$ in equation (2).

The solid curve in Figure 4 shows the result of our numerical calculation of the function $|e_1| = QmF_1(m)/2$ on the basis of equation (6); it corresponds to $Q \simeq 6.2$. This curve, which is remarkable, can be considered as a characteristic one. Fairly wide changes of the parameters N_t, $\mu\tau$, E_0, and Λ do not affect it seriously, provided the corresponding values of the quality factor Q lie within the range (5−7) which is most interesting for experiment. The vertical bars in Figure 4 show the spread of the results obtained for $N_t = (1{-}6) \times 10^{16}$ cm^{-3}, $\mu\tau = (0.7{-}4.2) \times 10^{-7}$ cm^2/V, $E_0 = (12{-}30)$ kV/cm, and $\Lambda = (10{-}50)$ μm. With increasing contrast this spread is decreasing. At $m = 1$ we have $|e_1| \simeq 0.62$, which agrees well with the above made analytic estimate. The close proximity of different curves means (i) that the quality factor Q determines the photorefractive nonlinear response in the whole range of the light contrast m and (ii) that the dependence of this response on Q is saturated for $Q \gg 1$.

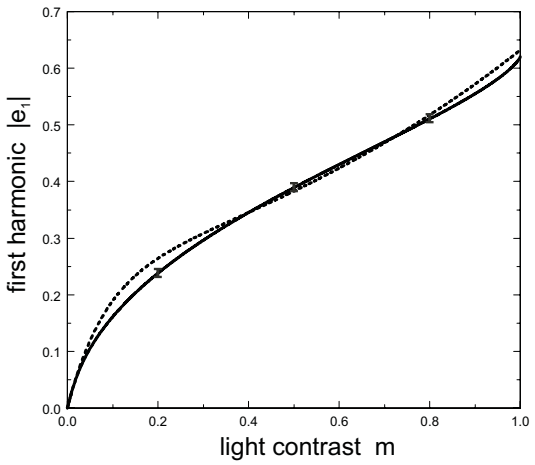

Fig. 4. Dependence of $|e_1|$ on the light contrast for $Q = 6.2$. The dotted curve corresponds to equation (9).

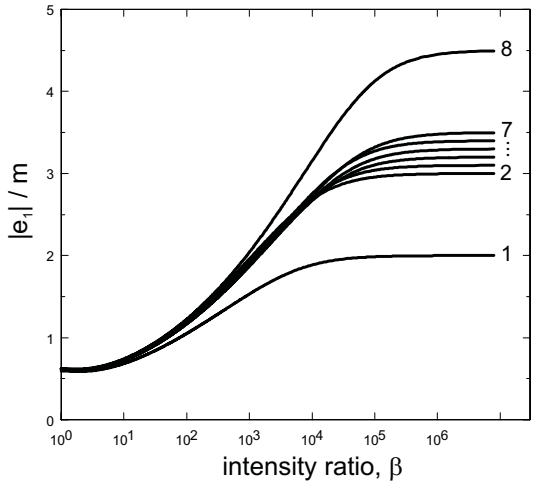

Fig. 5. Dependence of $|e_1|/m$ on β. The values of Q, $\mu\tau$ (in 10^{-7} cm^2/V), N_t (in 10^{16} cm^{-3}), Λ (in μm), and E_0 (in kV/cm) for the curves 1–8 are the following: 1 – (4.0, 1.63, 2.37, 40, 18); 2 – (6.0, 2.51, 2.38, 10, 18); 3 – (6.2, 4.23, 1.06, 20, 12); 4 – (6.4, 7.68, 6.6, 15, 30); 5 – (6.6, 1.48, 4.23, 25, 24); 6 – (6.8, 4.03, 1.44, 35, 14); 7 – (7.0, 3.34, 2,94, 50, 20); 8 – (9.0, 3.12, 2.94, 25, 20).

Instead of the contrast m it is often useful to employ the pump intensity ratio β. These quantities are coupled by the relation $m = 2\sqrt{\beta}/(1+\beta)$ with β ranging from 1 to ∞. Figure 5 shows the dependence $|e_1(\beta)|/m(\beta) = Q\,F(\beta)$ in a logarithmic scale for 8 different combinations $\mu\tau$, N_t, E_0, and Λ. For the curves 2–7 the quality factor ranges from 6 to 7, whereas the curves 1 and 6 are plotted for considerably smaller and bigger values of Q, respectively. For very large intensity ratios, $\log_{10}(\beta) > (4{-}5)$ (the low-contrast limit), each curve is characterized by a plateau on the level of $Q/2$; all the curves are clearly separated here. In the opposite case, $\log_{10}(\beta) \lesssim 2$ ($m \gtrsim 0.2$), the curves with $Q \geq 6$ practically coincide.

It is of interest also to compare the results of our numerical calculations with the expression used in [6,7] for fitting the numerical results and experimental data.

In our terms, this fit is equivalent to the representation of the function $e_1(m)$ in the form

$$e_1 = (-\mathrm{i}Q/2a)[1 - \exp(-am)]\exp(m)\ , \qquad (9)$$

where a is a fitting parameter. The dotted curve in Figure 4 shows the best fit of our numerical results, it corresponds to $a = 2.15\,Q$. One sees that the fitting function given by equation (8) reproduces fairly well the main features of the photorefractive AC-response. At the same time, the difference between the solid and dotted lines is noticeable for $m \approx 0.15$.

As seen from Figures 4 and 5, the whole contrast range can roughly be separated into two regions. The region $0 < m \lesssim 0.02$ ($\beta \gtrsim 10^4$) corresponds to the linear theory [3]. Here the fundamental amplitude E_1 grows rapidly with the contrast and the rate of spatial amplification of weak signals is extremely high, up to 10^2 cm^{-1}. In the second region, $0.1 \lesssim m < 1$, the growth of $E_1(m)$ is strongly saturated. This region is more appropriate for grating recording than for the spatial amplification purposes.

It should be underlined that the results exhibited are related to the case $Q \gtrsim (3-5)$ which is our prime interest. While the quality factor approaches unity, the effects of AC-enhancement fade quickly.

Apart from the fundamental harmonic e_1, responsible for beam-coupling effects, the first higher harmonics $e_2 = E_2/E_0$ and $e_3 = E_3/E_0$ are of practical interest. These harmonics can be measured with the help of auxiliary Bragg-matched light beams, they are important for characterization purposes. Since the function $e(x)$ is odd, all the higher Fourier harmonics are imaginary. Figures 6a and 6b show the dependences $|e_2(m)|$ and $|e_3(m)|$, respectively calculated for the same parameters as the solid curve of Figure 4. The function $|e_2(m)|$ peaks at $m \simeq 0.5$ and turns (as expected) to zero at $m = 1$. This dependence corresponds to the formation of the step-like field profile with increasing m, see Figure 3. Note that the initial (quadratic) interval of $|e_2(m)|$ is extremely narrow, $m \lesssim 0.02$, and the maximum expected value of $|E_{\mathrm{sc}}^{(2)}|$ is about $0.2E_0$. The spread of the curve in Figure 6a (shown by the vertical bars) is noticeably larger than that in Figure 4, especially in the region of relatively large m. The dependence $e_3(m)$ shown in Figure 6b looks quite different. It tends first to saturate at $m \simeq 0.2$ but experiences then a remarkable growth with m approaching unity. The maximum value of $E_{\mathrm{sc}}^{(3)}$ is about $0.4E_0$. Both the dependences of Figure 6 can be considered as the fingerprints of the AC-response in the sillenites.

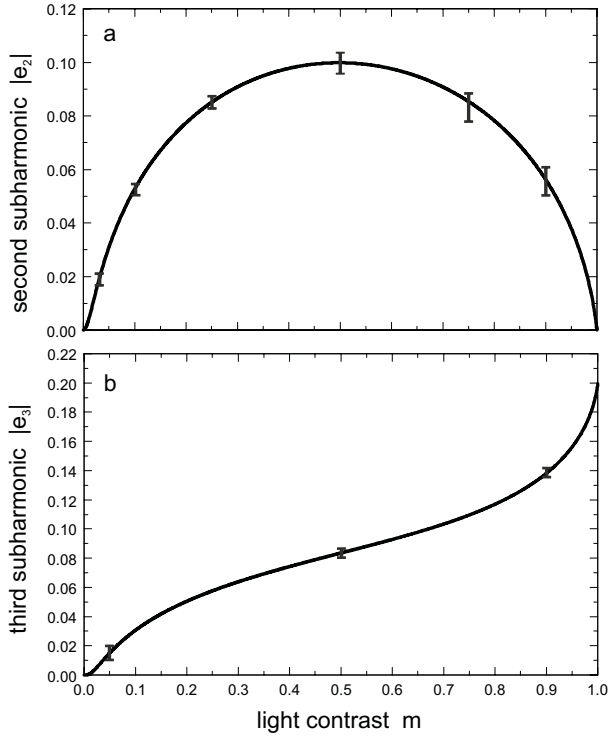

Fig. 6. Dependence of the second (a) and third (b) spatial subharmonics on the contrast m. The assumptions made are the same as for Figure 4.

4 Discussion

Let us comment first on the relationship between our results and the theoretical results presented in [6,7]. First of all we note that there is no serious contradiction between them. But there are, nevertheless, some differences. Partially, the parameters used in these papers correspond to the case $E_0 \lesssim (N_t k_b T/\epsilon\epsilon_0)^{1/2}$, which is of minor interest and lies outside the field of applicability of equation (6). Simulation of the time development of the charge density on the basis of the conventional one-species model restricted the possibilities of numerical experiments. In particular, the states attained were not fully stationary yet. It is not quite clear also whether the coordinate step used was always considerably smaller than the saturation length l_s. The mentioned circumstances can be the reason for minor quantitative distinctions in the cases where the approaches used can be compared.

Introduction of the quality factor Q has allowed us to represent the data on the fundamental harmonic in a fairly simple manner. This is especially true for the case $Q \gg 1$ which has become topical during the last years. The form of our results allows for their incorporation into the theory of vectorial beam coupling [20]. Lastly, we provide the reader with new data on the higher spatial harmonics $E_{2,3}$.

Several implications of the AC-response considered are also worth of discussion. The first one is how to measure the dependences $E_n(m)$ experimentally. In our opinion, the standard coupling geometries (the longitudinal, transverse, and diagonal), where the recording light beams propagate near the [110] (or [$\bar{1}$10]) axis, are not very useful for this purpose. The point is the coupling effects (involving also the polarization changes) can hardly be excluded even for relatively thin (∼1 mm) samples appropriate for the application of AC-fields. The most useful one seems to be the geometry used in [23,24] where the recording beams propagate nearby the [001] axis and testing Bragg-matched beams propagate nearby [110]. In this case,

the recorded space-charge field is not distorted by coupling effects and the minor remaining theoretical problem is to take into account the influence of optical activity and the AC-induced birefringence on the measured diffraction efficiency [26]. A similar technique was used to measure the higher harmonics of E_{sc} induced in the case of the co-called resonant DC-enhancement of the photorefractive response [17,18].

The next aspect is the influence of the m-dependence of the fundamental harmonic on the characteristics of two-beam coupling in the sillenites. It is important to realize that this coupling is essentially vectorial, *i.e.*, it cannot be reduced to the scalar one in the general case. The aforesaid is especially true with respect to the cases where the optical activity is essentially involved (which is, *e.g.*, always the case for BSO crystals). The use of the formulae of the scalar theory for fitting of the experimental dependences can result here in misleading conclusions. On the other hand, the use of the vectorial coupling theory (incorporating the polarization degrees of freedom) can result in qualitatively new polarization effects.

One of examples and applications of such effects is the linear detection of weak oscillating signals by means of a polarization filtering [27,28]. This new effect is feasible exclusively due to the vectorial character of beam coupling in cubic crystals. Its efficiency is expected to gain because of saturation of the dependence $E_1(m)$ in the region of large contrasts. The influence of coupling effects on the polarization linear detection is still an open problem.

One of the apparent manifestations of the AC-enhanced beam coupling is the light-induced (nonlinear) scattering in the sillenites [20–22]. Application of the vectorial theory to calculation of the scattering characteristics was based always on the expression (3) which is restricted to the low-contrast limit. The effects of saturation, that are clearly seen in experiment, were missing in these considerations. Development of the vectorial theory beyond the low-contrast limit is also a challenge which stems from experiment.

5 Conclusions

Using the governing equation for the space-charge field induced during 2W-coupling under an AC-field in the sillenites, we have analyzed numerically the dependences of the first Fourier harmonics, $E_{1,2,3}$ on the light contrast ranging from 0 to 1. We found out that these rather peculiar dependences are strongly controlled by the only scalar parameter – the quality (enhancement) factor Q. Comparison with the results of the previous studies is performed and the possibility for experimental detection of the theoretical predictions are discussed.

References

1. L. Solymar, D.J. Webb, A. Grunnet-Jepsen, *The Physics and Applications of Photorefractive Materials* (Claredon Press, Oxford, 1996)
2. M.P. Petrov, S.I. Stepanov, A.V. Khomenko, *Photorefractive Crystals in Coherent Systems* (Springer-Verlag, Berlin, 1991)
3. S.I. Stepanov, M.P. Petrov, Opt. Commun. **53**, 292 (1985)
4. C.S.K. Walsh, A.K. Powel, T.J. Hall, J. Opt. Soc. Am. B **7**, 288 (1990)
5. B.I. Sturman, M. Mann, J. Otten, K.H. Ringhofer, J. Opt. Soc. Am. B **10**, 1919 (1993)
6. J.E. Millerd, E.M. Garmire, M.B. Klein, B.A. Wechsler, F.P. Strohkendl, G.A. Brost, J. Opt. Soc. Am. B **9**, 1449 (1992)
7. G.I. Brost, J. Opt. Soc. Am. B **9**, 1454 (1992)
8. A.A. Kamshilin, E. Raita, A.V. Khomenko, J. Opt. Soc. Am. B **13**, 2536 (1996)
9. E. Raita, A.A. Kamshilin, T. Jaaskelainen, Opt. Lett. **23**, 1897 (1996)
10. C.A. Fuentes-Hernndez, A.V. Khomenko, Phys. Rev. Lett. **83**, 1143 (1999)
11. Ph. Delaye, L.A. de Montmorillon, G. Roosen, Opt. Commun. **118**, 154 (1995)
12. A.A. Kamshilin, Y. Iida, S. Ashihara, T. Shimura, K. Kuroda, Appl. Phys. Lett. **74**, 2575 (1999)
13. A.A. Kamshilin, K. Paivasaari, M. Klein, B. Pouet, Appl. Phys. Lett. **77**, 4098 (2000)
14. G.F. Calvo, B.I. Sturman, F. Agullo-Lopez, M. Carrascosa, Phys. Rev. Lett. **84**, 3839 (2000)
15. G. Fernandez, B. Sturman, F. Agullo-Lopez, M. Carrascosa, Phys. Rev. Lett. 2002 (accepted)
16. P. Refregier, L. Solymar, H. Rajbenbach, J.-P. Huignard, J. Appl. Phys. **58**, 45 (1985)
17. T.E. McClelland, D.J. Webb, B.I. Sturman, M. Mann, K.H. Ringhofer, Opt. Commun. **113**, 371 (1995)
18. T.E. McClelland, D.J. Webb, B.I. Sturman, E. Shamonina, M. Mann, K.H. Ringhofer, Opt. Commun. **131**, 315 (1996)
19. A. Marrakchi, R.V. Johnson, A.R. Tanguay, J. Opt. Soc. Am. B **3**, 321 (1986)
20. B.I. Sturman, E.V. Podivilov, K.H. Ringhofer, E. Shamonina, V.P. Kamenov, E. Nippolainen, V.V. Prokofiev, A.A. Kamshilin, Phys. Rev. E **60**, 3332 (1999)
21. H. Touvinen, A.A. Kamshilin, J. Jaaskelainen, J. Opt. Soc. Am. B **14**, 3383 (1997)
22. V.P. Kamenov, E. Shamonina, K.H. Ringhofer, E. Nippolainen, V.V. Prokofiev, A.A. Kamshilin, Phys. Rev. E **62**, 2863 (2000)
23. T.E. McClelland, D.J. Webb, B.I. Sturman, K.H. Ringhofer, Phys. Rev. Lett. **73**, 3082 (1994)
24. H.C. Pedersen, D.J. Webb, P.M. Johansen, J. Opt. Soc. Am. B **15**, 2439 (1998)
25. G.B. Whitham, *Linear and nonlinear waves* (Willey-Interscience, NY, 1974)
26. B.I. Sturman, D.J. Webb, R. Kowarschik, E. Shamonina, K.H. Ringhofer, J. Opt. Soc. Am. B **11**, 1813 (1994)
27. K. Paivasaari, A.A. Kamshilin, V.V. Prokofiev, B.I. Sturman, G.F. Calvo, M. Carrascosa, F. Agullo-Lopez, J. Appl. Phys. **90**, 3135 (2001)
28. G.F. Calvo, B.I. Sturman, F. Agulló-López, M. Carrascosa, A.A. Kamshilin, K. Paivasaari, J. Opt. Soc. Am. B **17** (2002)
29. N. Wolffer, P. Gravey, R. Coquill, J. Appl. Phys. **78**, 6375 (1995)
30. L. Boutsikaris, F. Davidson, Opt. Commun. **105**, 411 (1994)